# MR imaging: normal and invaded cavernous sinus studied with and without Gd-DTPA

M. KOMIYAMA[1], T. YASUI[1], M. BABA[1], A. HAKUBA[2], S. NISHIMURA[2], Y. NEMOTO[3], and Y. INOUE[3]

[1] Department of Neurosurgery, Baba Memorial Hospital, Sakai, Osaka, and Departments of [2] Neurosurgery and of [3] Radiology, Osaka City University Medical School, Osaka, Japan

Clinical efficacy of MR imaging for demonstrating the normal and abnormal cavernous sinus (CS) was evaluated. Six normal CS and six CS invaded by pituitary adenomas were studied with a 0.5 T MR scanner using T 1-weighted SE sequences. Furthermore, all normal CS and one invaded CS were studied with gadolinium (Gd)-DTPA. The internal carotid artery (ICA) was shown as low intensity and not enhanced with Gd-DTPA. Venous flow in the CS could be divided into two compartments, *i.e.*, rapid and slow flows. Both flows were demonstrated as lower intensity than the white matter and higher than ICA. Slow flow was markedly enhanced with Gd-DTPA, but rapid flow was enhanced to a lesser degree than the slow. Invasion of the CS was demonstrated as follows: the engulfment of the ICA by the tumor; lack of relatively low intensity of venous flow; the extension of the tumor to the lateral wall of the CS; and the marked displacement of the ICA. MR imaging was useful for the recognition of the blood flows and the tumor invasion in the CS.

## Introduction

Recent advances in magnetic resonance (MR) imaging have brought a new era in diagnostic neuroradiology. Most advantages are due to lack of ionizing radiation, high contrast resolution, lack of artifacts from the adjacent bony structures, and multiplanar imaging capabilities. Pituitary adenomas are readily diagnosed with MR imaging since it enables the recognition of the suprasellar extension of the tumors and visual pathways which are difficult to visualize with X-ray computed tomography (CT) [2, 7, 9, 11]. The recognition of a tumor invasion of the cavernous sinus (CS) still remains as a diagnostic problem even with high resolution X-ray CT with contrast media. Here, normal CS and CS invaded by pituitary adenomas were studied and visualization of the CS was described and the clinical efficacy of MR for CS pathology was discussed.

## Patients and methods

Six brain tumor patients (group A), who had a normal CS clinically and radiologically, and six pituitary adenoma patients (group B), 4 of whom were operated on and diagnosed histopathologically and 2 of whom were diagnosed clinically and radiologically, underwent MR examinations. In

**Table 1.** Case Summary

Group A: Normal cavernous sinus

| Case no. | Age | Sex | Diagnosis |
|---|---|---|---|
| 1 | 35 | M | Occipital glioma |
| 2 | 50 | M | Frontal glioma |
| 3 | 34 | M | Frontal glioma |
| 4 | 35 | F | Falx meningioma |
| 5 | 20 | F | Parietal cavernoma |
| 6 | 48 | F | Frontal metastasis |

Group B: Cavernous sinus invaded by pituitary adenomas

| Case no. | Age | Sex | Producing hormone | CS invasion on MRI | | Operation | CS invasion confirmed | |
|---|---|---|---|---|---|---|---|---|
| 7 | 54 | M | non | R − | L + | + | R ? | L ? |
| 8 | 55 | M | non | R ? | L + | + | R ? | L ? |
| 9 | 63 | M | non | R + | L − | − | − | − |
| 10 | 79 | F | non | R + | L − | − | − | − |
| 11 | 24 | F | GH | R ? | L + | + | R − | L + |
| 12 | 37 | F | PRL | R + | L − | + | R + | L − |

*CS* cavernous sinus. In cases 7 and 8, CS were not explored group B, in two pituitary adenoma cases (cases 11 and 12), CS invasion by pituitary adenomas was confirmed by surgery and in the remaining 4 cases CS invasion was diagnosed clinically and/or radiologically. The case summary is presented in Table 1. The MR scanner was a 0.5 T superconductive MR system (Picker International, Cleveland, OH). T 1-weighted spin echo (SE) sequences, i.e., SE 600–1,000/40 (repetition time/echo time, msec) were used. Slice thickness was 1.0 cm and coronal images were obtained. The data collection matrix was 256 by 256 and averaging was carried out once. In all patients in group A and in case 11 in group B, the CS was examined by intravenous administration of gadolinium-diethylenetriamine pentaacetic acid (Gd-DTPA) in a dose of 0.1 mmol/kg. MR signal intensity is expressed as intensity relative to the normal white matter.

## Results

### *Normal CS images*

Arterial flow in the internal carotid artery (ICA) (Fig. 1) was always demonstrated as low signal intensity on both plain and enhanced images with Gd-DTPA. Venous canals were recognized as two compartments. Both compartments showed lower signal intensity than the normal white matter and higher than the ICA. However, one was enhanced markedly with Gd-DTPA and the other was enhanced to a lesser degree. Although neural structures in the CS were not always visualized, enhanced images with Gd-DTPA were superior than nonenhanced images for the demonstration of neural structures in the CS.

### *Images of CS invaded by pituitary adenomas*

Pituitary adenomas showed isointensity or slightly high intensity compared with the normal white matter (Figs. 2, 3, 4, 5). CS invasion by pituitary adenomas was demonstrated as follows: the engulfment of the ICA by the tumor; lack of relatively low signal intensity of venous flow; the extension of the tumor to the lateral wall of the CS; and the marked displacement of the ICA. In case 11, the pituitary adenoma was enhanced heterogeneously with Gd-DTPA and the tumor invading the CS was also enhanced.

## Discussion

In MR imaging of the normal CS, arterial flow in the ICA usually shows low or negligible signal intensity due to the high velocity of the blood flow [10] unless the flow velocity is low due to stenosis or obliteration of the ICA.

Angiographically, there are two ways to demonstrate the venous canals in the CS. One is carotid angiography and the other venography. As regards venography, there are two methods, i.e., orbital venography and jugular venography. It is of great interest that opacification of venous canals in the CS is different between the venous phase of carotid angiography and venography. Visualized venous canals in the CS are always larger in venography than in carotid angiography. We think that there are principally two kinds of venous flows in the CS, *i.e.*, rapid flow and slow flow. In the venous phase of carotid angiography, only rapid venous flow is visualized and slow flow in scarcely visualized. However, in venography both rapid and slow flows are visualized. This is the reason why there are differences regarding sizes of opacified venous canals between carotid angiography and venography.

In MR images, these two venous flows showed relatively low signal intensities, which were dependent on their flow velocities and imaging parameters (pulse sequences, repetition times, and echo times). They were easily recognized as relatively low intensity on T 1-weighted SE images. However, they were not absolutely low or of negligible intensity like an arterial flow in the ICA since they were enhanced by the flow-related enhancement (paradoxical enhancement) [3, 10] even without Gd-DTPA. Gd-DTPA has the property of reducing the relaxation times (T 1 and T 2) of surrounding protons due to proton relaxation enhancement [4, 14]. Its enhancement effect on images is very similar to that of iodinated contrast enhancement in X-ray CT. Venous flows imaged with Gd-DTPA show various signal intensities due to the combination of flow-related enhancement and proton relaxation enhancement. Slow venous flow was always enhanced with Gd-DTPA due to these two enhancement mechanisms, while rapid venous flow was enhanced to a lesser degree than slow flow.

Pituitary adenomas showed isointensity or sightly high intensity in comparison to the normal white matter and were enhanced with Gd-DTPA. Slow venous flow showed lower intensity than those of pituitary adenomas. Intracavernous nerve structures were not identified probably due to the thickness of the image slices, so visualization of neural structures in the CS was poor and is not discussed extensively in this paper. Gd-DTPA enhanced the pituitary glands, stalks, and venous flows in the CS, but did not enhance the optic chiasm and nerves in the CS. Gd-DTPA could facilitate demonstrating venous flows and nerve structures in the CS.

It is difficult to diagnose invasion of the CS by pituitary adenomas definitely at present. In order to evaluate CS pathology with X-ray CT, the CS is studied with high resolution, thin-section, and direct coronal

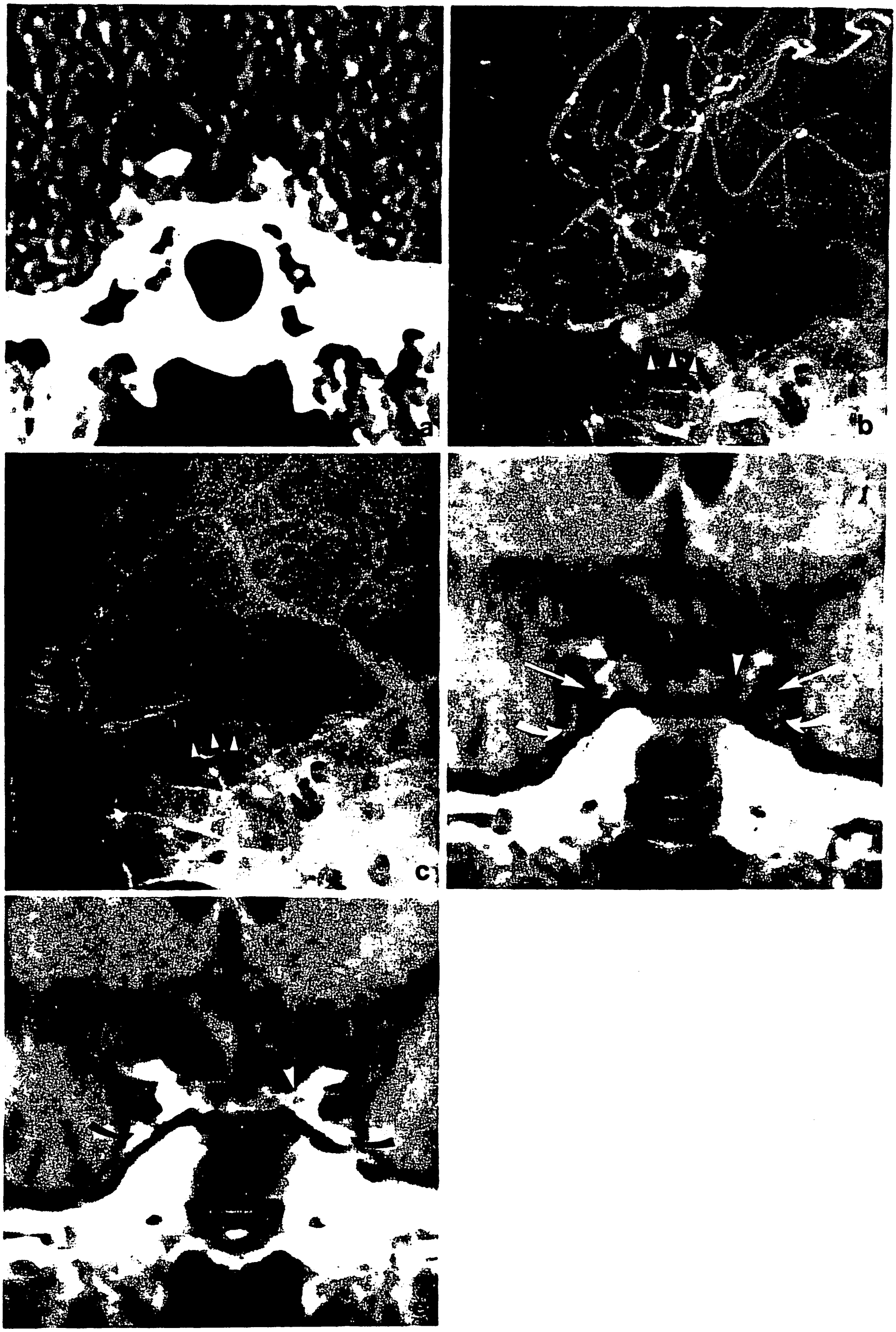
a
b
c

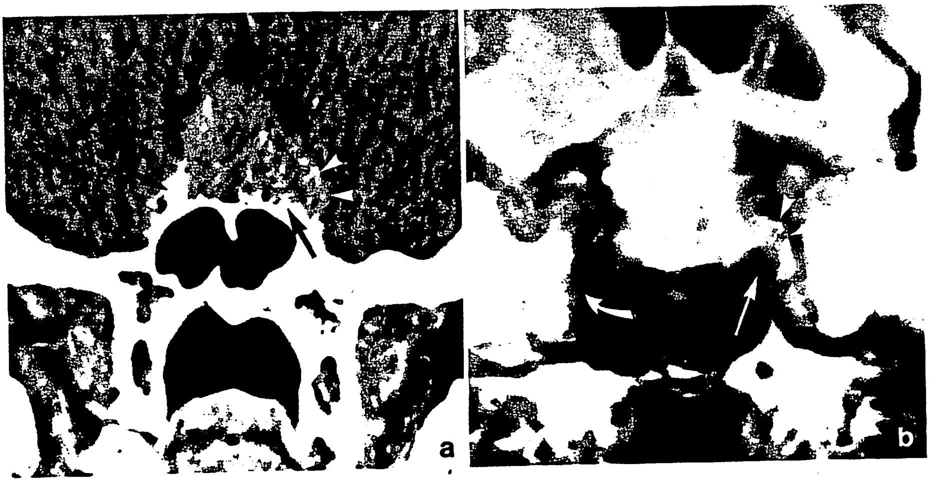


**Fig. 2.** A 54-year-old male with nonfunctioning pituitary adenoma (case 7). **a** Enhanced CT demonstrates the high density of internal carotid arteries (arrows). Bulging of the left cavernous sinus may be noted (arrowheads). **b** T 1-weighted SE image. Left carotid artery (straight arrow) is displaced infero-laterally and engulfed by the tumor. The tumor extends to the lateral wall of the cavernous sinus (arrowheads). Relatively low intensity of venous flow (curved arrow) is noted on the right side and it is not observed on the left side due to the invasion of the tumor

techniques, in which intravenous bolus and/or continuous administration of iodinated contrast media is mandatory [6, 8, 12, 13]. With these techniques, the CS is markedly enhanced and pituitary adenomas usually show slightly less enhancement than the CS. Invasion of pituitary adenomas into the CS was demonstrated in X-ray CT as follows: CS expansion; visible encasement of the ICA; intracavernous cranial nerve compression, obliteration, or displacement; invasion of the lateral wall of the CS, and diffuse

---

**Fig. 1.** Normal cavernous sinus in an occipital glioma patient (case 1). **a** Enhanced CT can not demonstrate internal carotid arteries. **b** Arterial phase of the left carotid angiography. Arrowheads indicate internal carotid artery. **c** Venous phase of the left carotid angiography. Arrowheads indicate rapid venous flow in the cavernous sinus. **d** T 1-weighted SE image without Gd-DTPA. Carotid arteries are clearly demonstrated as a low intensity area (straight arrows) and rapid venous flow is demonstrated just medial to the left internal carotid artery (arrowhead) in the cavernous sinus as a slightly low intensity area. The relatively low signal intensity of slow venous flows by may noted (curved arrows). **e** T 1-weighted SE image with Gd-DTPA. Slow venous flows are markedly enhanced (curved arrows), whereas fast venous flow (arrowhead) shows lower signal intensity than slow venous flow

**Fig. 3.** A 55-year-old male with nonfunctioning pituitary adenoma (case 8). T 1-weighted SE image. The internal carotid artery (arrows) is markedly displaced superiorly and the tumor extends to the lateral wall of the cavernous sinus (arrowheads)

bone destruction [1]. However, it is sometimes difficult to diagnose the invasion of pituitary adenomas into the CS and it is impossible to differentiate rapid and slow flows in the CS with X-ray CT even with the above-mentioned techniques.

To obtain coronal images, MR imaging can be performed with the neck of the patient in the neutral position. This is a great advantage over X-ray CT. Although Daniels et al. [5] demonstrated good MR images of the normal CS, there has not been an extensive description of CS invasion by pituitary adenomas so far. CS invasion by pituitary adenomas is strongly suggested by the following findings: the engulfment of the ICA by the tumor; lack of relatively low signal intensity of venous flow on T 1-weighted SE images; the extension of the tumor to the lateral wall of the CS; and marked displacement of the ICA. These findings help us to recognize CS invasion by pituitary adenomas.

In conclusion, MR imaging is useful for the recognition of tumor invasion of the CS as well as for the demonstration of the relationships between the visual pathways and the tumor, and suprasellar extension of the tumor. MR imaging can give us a lot of information for the determination of the appropriate therapy for pituitary adenomas.

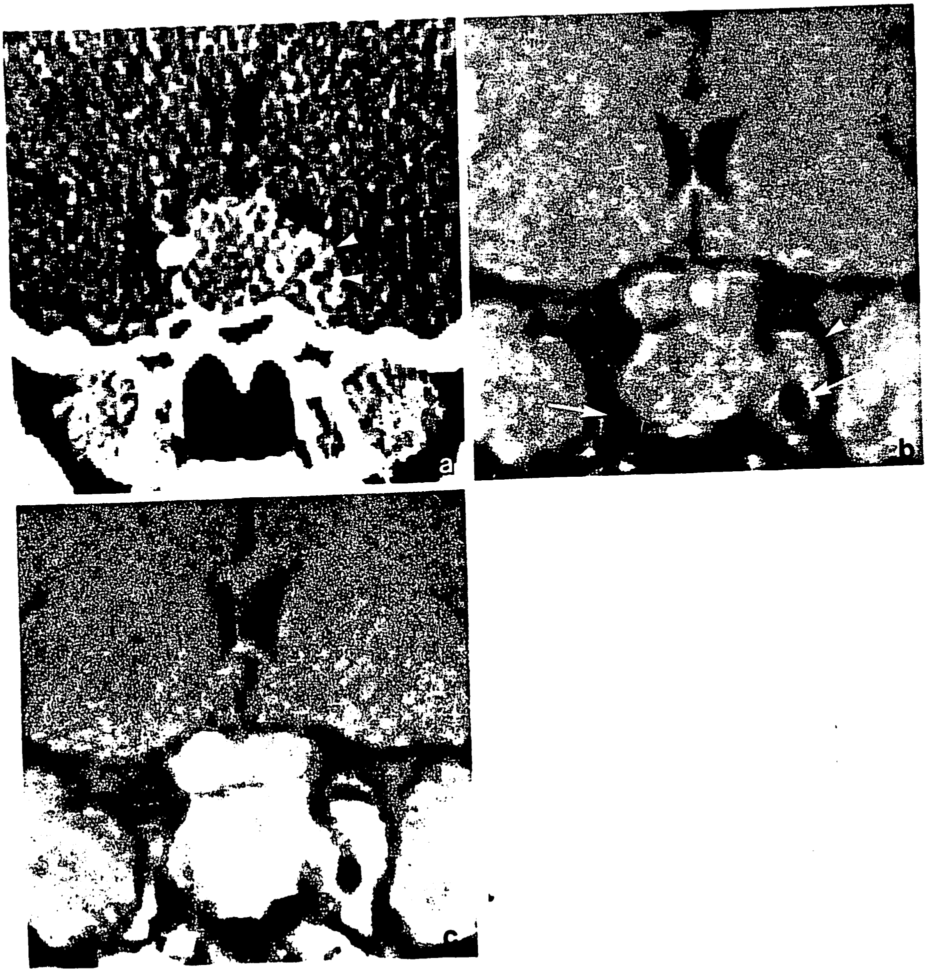


**Fig. 4.** A 24-year-old female with human growth hormone producing pituitary adenoma (case 11). **a** Enhanced CT demonstrates the bulging of the left cavernous sinus (arrowheads). However, it is difficult to differentiate internal carotid arteries from the tumor. **b** T 1-weighted SE image without Gd-DTPA. Internal carotid arteries are clearly demonstrated as low intensity area (arrows). The left internal carotid artery is markedly displaced laterally and engulfed by the tumor. The tumor extends to the left lateral wall of the cavernous sinus (arrowhead). **c** T 1-weighted SE image with Gd-DTPA. The tumor is enhanced with Gd-DTPA

**Fig. 5.** A 37-year-old female with prolactinoma (case 12). T 1-weighted SE image. The tumor extends to the right lateral wall of the cavernous sinus (arrow) and engulfs the right internal carotid artery, which is displaced laterally. Lack of relatively low intensity of venous flow is noted on the right side

## References


1. Ahmadi J, North CM, Segall HD, Zee CS, Weiss MH (1985) Cavernous sinus invasion by pituitary adenomas. ANJR 6: 893–898
2. Bilaniuk LT, Zimmerman RA, Wehrli FW, Snyder PJ, Goldberg HI, Grossman RI, Bottomley PA, Edelstein WA, Glover GH, MacFall JR, Redington RW (1984) Magnetic resonance imaging of pituitary lesions using 1.0 to 1.5 T field strength. Radiology 153: 415–418
3. Bradley WG, Waluch V, Lai KS, Fernandez EJ, Spalter C (1984) The appearance of rapidly flowing blood on magnetic resonance images. AJR 143: 1167–1174
4. Carr DH, Brown J, Bydder GM, Steiner RE, Weinmann HJ, Speck U, Hall AS, Young IR (1984) Gadolinium-DTPA as a contrast agent in MRI: initial clinical experience in 20 patients. AJNR 143: 215–224
5. Daniels DL, Pech P, Mark L, Pojunas K, Williams AL, Haughton VM (1985) Magnetic resonance imaging of the cavernous sinus. AJR 6: 187–192
6. Hasso AN, Aubin ML, Pop PM, Bar D, Thompson JR, Becker TS, Hinshaw DB Jr, Vignaud J (1982) High resolution thin section computed tomography of the cavernous sinus. RadioGraphics 2: 83–100
7. Hawkes RC, Holland GN, Moore WS, Corston R, Kean DM, Worthington BS (1983) The application of NMR imaging to the evaluation of pituitary and juxtasellar tumors. AJNR 4: 221–222

8. Kline LB, Acker JD, Post MJD, Vitek JJ (1981) The cavernous sinus: A computed tomographic study. AJNR 2: 299–305
9. Lee BCP, Deck MDF (1985) Sellar and juxtasellar lesion detection with MR. Radiology 157: 143–147
10. Mills CM, Brant-Zawadzki M, Crooks LE, Kaufman L, Sheldon P, Norman D, Bank W, Newton TH (1984) Nuclear magnetic resonance: principles of blood flow imaging. AJR 142: 165–170
11. Oot R, New PFJ, Buonanno FS, Pykett IL, Kistler P, Delapaz R, Davis KR, Taveras JM, Brady TJ (1984) MR imaging of pituitary adenomas using a prototype resistive magnet: preliminary assessment. AJNR 5: 131–137
12. Swartz JD, Russell KB, Basile BA, O'Donnell PC, Popky GL (1983) High resolution computed tomography of the intrasellar contents: normal, near normal and abnormal. RadioGraphics 3: 228–247
13. Taylor S (1982) High resolution computed tomography of the sella. Radiol Clin North Am 20: 207–236
14. Weinmann HJ, Brasch RC, Press WR, Wesbey GE (1984) Characteristics of gadolinium-DTPA complex: a potential NMR contrast agent. AJR 142: 619–624